Bioorganic & Medicinal Chemistry Letters 18 (2008) 4844–4848

Contents lists available at ScienceDirect

Bioorganic & Medicinal Chemistry Letters

journal homepage: www.elsevier.com/locate/bmcl

Evaluation of indazole-based compounds as a new class of potent KDR/VEGFR-2 inhibitors

David Bauer [a,*], Douglas A. Whittington [b], Angela Coxon [c], James Bready [c], Shawn P. Harriman [d], Vinod F. Patel [a], Anthony Polverino [e], Jean-Christophe Harmange [a]

[a] Department of Medicinal Chemistry, Amgen, Inc., One Kendall Square, Building 1000, Cambridge, MA 02139, USA
[b] Department of Molecular Structure, Amgen, Inc., One Kendall Square, Building 1000, Cambridge, MA 02139, USA
[c] Department of Oncology Research, Amgen, Inc., One Amgen Center Drive, Thousand Oaks, CA 91320, USA
[d] Department of Pharmacokinetics and Drug Metabolism, Amgen, Inc., One Kendall Square, Building1000, Cambridge, MA 02139, USA
[e] Department of Oncology Research, Amgen, Inc., 1201 Amgen Court West, Seattle, WA 98119, USA

ARTICLE INFO

Article history:
Received 2 May 2008
Revised 18 July 2008
Accepted 21 July 2008
Available online 24 July 2008

Keywords:
KDR inhibitor
VEGFR-2 inhibitor
Kinase inhibitor

ABSTRACT

A novel class of potent and selective inhibitors of KDR incorporating an indazole moiety **1** is reported. The discovery, synthesis, and structure–activity relationships of this series of inhibitors have been investigated. The most promising compounds were also profiled to determine their pharmacokinetic properties and evaluated in a VEGF-induced vascular permeability assay.

Angiogenesis, the formation of new blood vessels from existing vasculature, is a critical process in tumor growth.[1] Among the many pro-angiogenic factors, vascular endothelial growth factor (VEGF) has been identified as the most important regulator of tumor angiogenesis.[2] Endothelial cell proliferation and migration, two crucial steps in angiogenesis, are mediated through a specific VEGF receptor, the kinase insert domain-containing receptor (KDR or VEGFR-2). Inhibition of KDR kinase activity by small molecules has been shown to be a very promising way to interdict this VEGF pathway in human cancers. More specifically two small molecule inhibitors of KDR, Sutent (sunitinib)[3] and Nexavar (sorafenib tosylate),[4] have recently been approved for patients with gastrointestinal stromal tumors (GIST) and advanced renal cell carcinoma, respectively.

Aryl-aminonaphthyl compounds **1** are potent inhibitors of VEGF receptor tyrosine kinase.[5] However, *N*-hydroxy-1-aminonaphthalene, a known metabolite of the 1-aminonaphthalene, has been described as mutagenic and carcinogenic.[6] Consequently, we flagged the 1-aminonapthyl core as a possible concern and looked for a replacement. In our search for a surrogate ring system, we also considered increasing the polar surface area and decreasing the Log*P* to lean toward molecules with projected improved physicochemical properties. Herein, we describe the structure–activity relationship (SAR) for a novel series of indazoles **2**, which possess good in vitro potency, selectivity, and pharmacokinetic properties (Scheme 1).

Compounds were synthesized by the route outlined in Scheme 2. 1-Methyl-3 amino-6-hydroxyindazole **3** can be prepared on multi-gram scale by reaction of 2-fluoro-4-hydroxybenzonitrile with methylhydrazine. The aminohydroxyindazole **3** was then reacted with 4-chloro-6,7-dimethoxyquinoline[7] under basic conditions to afford the biaryl ether intermediate **4**. *N*-Arylation using the Buchwald phosphine[8] or reductive amination then, respectively, afforded the desired compounds **5** or **6**.

Table 1 summarizes SAR[9] and *c*Log*P*[10] for a selection of alkyl and aryl substituents. These compounds had predicted Log*P* one log unit lower than their analogs in the aminonaphthalene series (e.g., compare compounds **5a** with **1a** [*c*Log*P* = 7.0] and **5b** with **1b** [*c*Log*P* = 7.1]). The alkyl amine derivatives explored were weak KDR inhibitors. Although phenyl substituent led to potent KDR inhibitors in the aminonaphthyl series (compound **1a**), only weak inhibition was achieved in the indazole series (compound **5a**). Addition of an electrodonating group at the *meta*- (**5b**) and *para*-position (**5c**) of the phenyl group did not change the inhibitory activity. However, a significant potency improvement resulted from introduction of a more lipophilic trifluoromethyl substituent (compound **5d**). As we have previously observed, replacement of the naphthyl core by a less lipophilic scaffold tends to result in a loss of potency, which may be countered by utilizing lipophilic

* Corresponding author. Tel.: +1 617 444 5023; fax: +1 617 577 9822.
E-mail address: dbauer@amgen.com (D. Bauer).

0960-894X/$ - see front matter © 2008 Elsevier Ltd. All rights reserved.
doi:10.1016/j.bmcl.2008.07.080

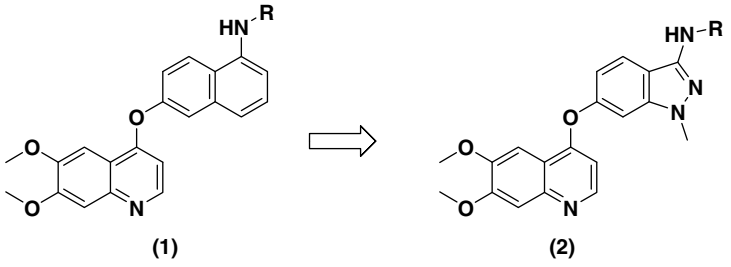

(1a) R=Ph, KDR IC_{50} = 2nM (cLogP = 7.0)
(1b) R=2-methoxyphenyl, KDR IC_{50} = 1nM (cLogP = 7.1)

Scheme 1.

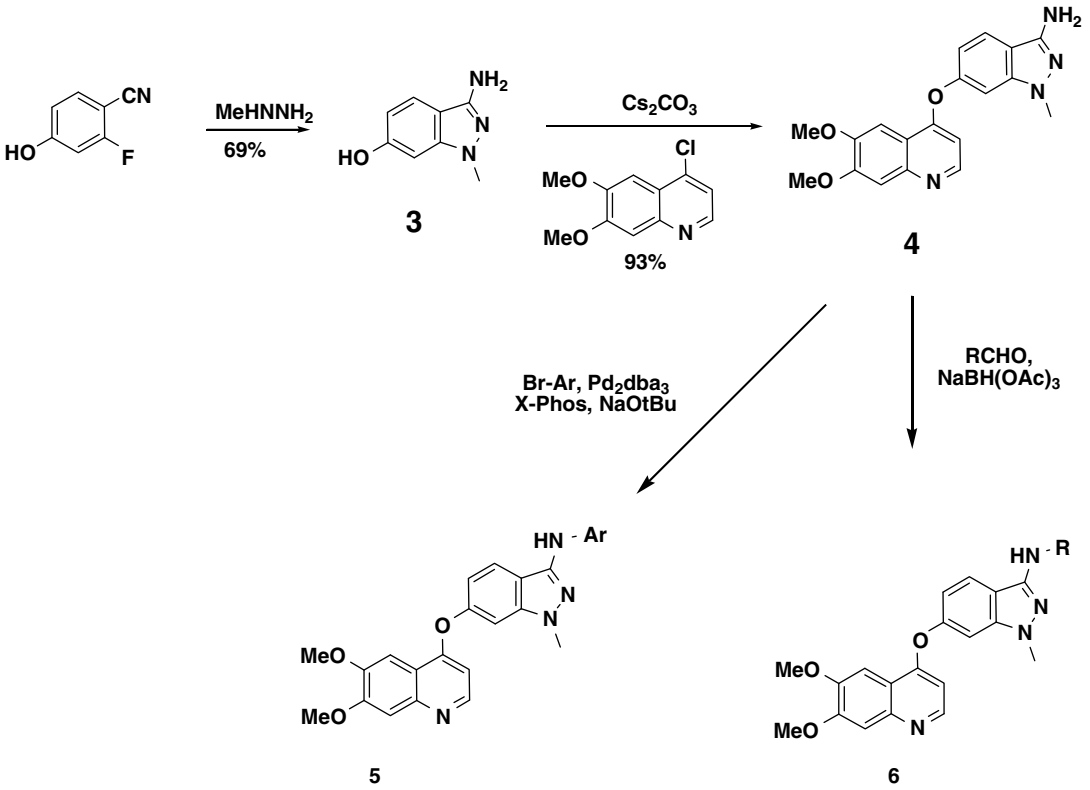

Scheme 2.

aromatic substituents.[11] This strategy appears to be a valid solution here also. The introduction of a methylene group between the indazole core and the phenyl group had a similar beneficial effect (compound **6d**).

Consequently, an amide linkage was next explored (Table 2). The aminocarbonyl tether provided compounds with high affinity for the enzyme as illustrated by compound **7d**: compared with the parent compound **5c**, a 50-fold increase of enzyme inhibition was observed. A 20-fold improvement in enzyme inhibition was also observed with compound **7e** compared with the parent compound **5d**.

These compounds were also evaluated in our whole cell assay by measuring the inhibition of VEGF-stimulated cellular proliferation of human umbilical vascular endothelial cells (V-HUVEC).[9] The shift in potency measured in the cellular assay compared with that observed in the enzyme was relatively small (about 10-fold) with the notable exception of compounds **7e** and **7i**, which exhibited a 30-fold shift. This difference may not be explained solely by compromised cell permeability resulting from the high lipophilicity of these compounds ($c\mathrm{Log}P$ = 5.7 and 6.6, respectively), as compound **7j** ($c\mathrm{Log}P$ = 5.7) exhibited only a threefold shift. To measure the selectivity of this series in a cellular assay, the compounds were evaluated in a basic fibroblast growth factor (bFGF)-driven HUVEC (F-HUVEC) proliferation assay.[12] All the compounds tested exhibited a very high level of selectivity.[13]

An X-ray co-crystal structure of amide **7j** bound to the ATP-site of KDR was obtained (Scheme 3).[14] The quinoline makes a key hydrogen bond to the backbone NH of the linker residue, Cys 919 (3.1 Å). An additional hydrogen bond between the quinoline and the backbone CO of the linker Cys 919 (3.4 Å) also contributes to the interaction of the compound with the linker region of KDR. The amide moiety of **7j** interacts with the protein through two hydrogen bonds; the NH forms a hydrogen bond with Glu 885 while the carbonyl interacts with Asp 1046. The substituted phenyl ring pushes deep into the extended hydrophobic pocket formed by the reorganization of Phe 1047 (of the Asp 1046, Phe 1047, Gly 1048 triad, the 'DFG' motif) to induce the 'DFG-out' conformation.[15] These hydrophobic interactions account for a significant

Table 1
KDR potency (IC_{50}, μM) for amines variations of the indazole

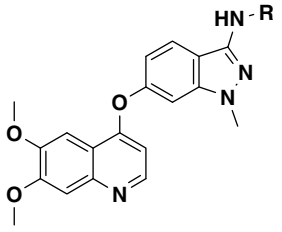

	R	KDR	*c*Log*P*
4	H	1.70	3.1
6a	Et	0.37	4.4
6b	*n*-Pr	1.11	4.9
6c	*n*-Bu	0.80	5.4
5a		0.27	5.8
5b	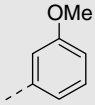	0.23	5.8
5c	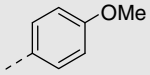	0.16	5.8
5d	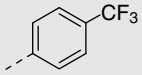	0.07	6.9
6d	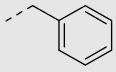	0.06	5.3

proportion of the binding affinity. Compounds having a smaller substituent at this position bind more weakly (e.g., cyclopropyl **7a**, IC_{50} = 0.344 μM), confirming the importance of occupying the extended hydrophobic pocket as a means of enhancing potency. The amide moiety serves as a rigid extender to place the terminal aryl ring fully into the extended hydrophobic pocket. In addition, the amide makes favorable hydrogen bond interactions using both the NH and the carbonyl lone pair.

Recognizing that a urea linkage could potentially allow the aryl substituent to occupy the same region of space, the urea derivatives **8a–d** were accessed (Table 3). Gratifyingly, these compounds were very potent at inhibiting KDR. Compounds **8a**, **8c**, and **8d** also displayed good potency at the cellular level. The selectivity over F-HUVEC remained high for all compounds.[13]

Encouraged by the excellent potency and high selectivity of this series of compounds, the pharmacokinetic properties were examined in vivo in male Sprague–Dawley rats, administered by both intravenous (iv) and oral (po) routes (Table 4).[16] Clearance was low to moderate for all four compounds. Compounds **7h**, **7j**, and **8a** exhibited acceptable half-lives. Although **8a** had a $t_{1/2}$ of 4.3 h, it was compromised by poor bioavailability and low exposure. Compound **7h** was also rejected due to its poor oral pharmacokinetic properties (low exposure and bioavailability). Compound **7j**, however, showed favorable pharmacokinetic properties with good bioavailability and satisfactory oral exposure.

Compound **7j** was chosen for further profiling. The selectivity profile was explored across a range of tyrosine kinases (Table 5). Compound **7j** showed high selectivity for KDR inhibition (IC_{50} = 0.001 μM); all the other kinases tested in the panel returned inhibition values at least 45-fold higher.

Table 2
Investigation of an amide linkage (IC_{50}, μM)

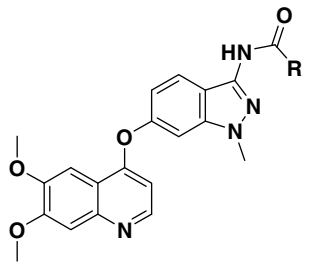

	R	KDR	V-HUVEC
7a		0.344	—
7b	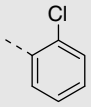	0.008	—
7c		0.005	0.061
7d	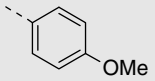	0.003	0.032
7e		0.003	0.079
7f	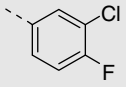	0.003	0.009
7g	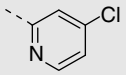	0.002	0.027
7h	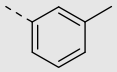	0.002	0.002
7i	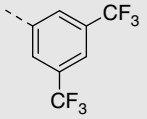	0.002	0.058
7j	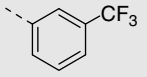	0.001	0.009

Based on V-HUVEC potency (IC_{50} = 9 nM), promising pharmacokinetics, and its high selectivity over other kinases, the in vivo activity of compound **7j** was evaluated in a VEGF-induced vascular permeability assay.[17] Briefly, cells over-expressing murine VEGF or control were combined with Matrigel and injected subcutaneously into athymic nude mice. Twenty-four hours later, the animals were administered either drug or vehicle. Vascular permeability was assessed 6 h after administration of compound. In addition, a satellite group of animals (n = 2) were dosed with compound, and blood samples were harvested at 6 h to determine plasma concentration of compound. The results obtained for mice dosed with **7j** are presented in Scheme 4. Although there was no response at 3 mg/kg, significant inhibition of vascular permeability at 10 and 30 mg/kg (plasma concentration: 181 and 347 ng/mL, respectively) was ob-

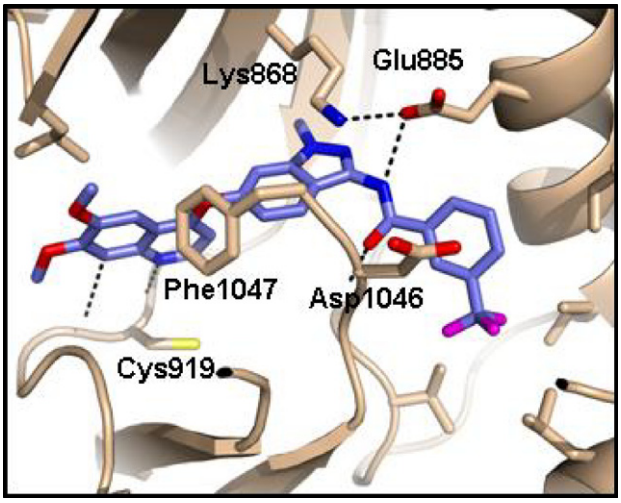

Scheme 3. Key binding interactions with compound **7j** (purple) with KDR.

Table 3
Investigation of a urea linkage (IC_{50}, μM)

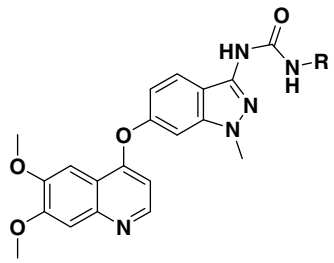

	R	KDR	V-HUVEC
8a		0.002	0.006
8b	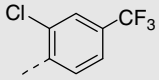	0.008	1.15
8c	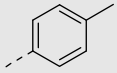	0.002	0.003
8d	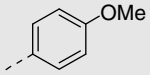	0.001	0.007

Table 4
Pharmacokinetic parameters in male Sprague–Dawley rats

	CL (L/h/kg)	V_{ss} (L/kg)	$t_{1/2}$ (h)	F (%)	$AUC_{0-\infty}$ (ng h/mL)
7f	1.3	2.1	1.5	—	—
7h	1.2	2.4	2.7	12	153
7j	0.7	1.4	2.2	46	1528
8a	0.4	2.0	4.3	2	121

Compounds were formulated in 100% DMSO for iv dosing and 100% Ora-Plus for po dosing.

served, demonstrating that compound **7j** inhibited VEGF-induced vascular permeability in a dose-dependent fashion.

In conclusion, we successfully replaced the 1-aminonaphthyl core by a 3-aminoindazolyl core as illustrated by the selectivity,

Table 5
Kinase selectivity (IC_{50}, μM)

Enzyme inhibition			
Aurora 1	0.045	PI3K	3.25
Tie-2	0.121	cMet	3.32
Aurora 2	0.764	JAK3	25,000
p38α	1.65	JNK2	25,000

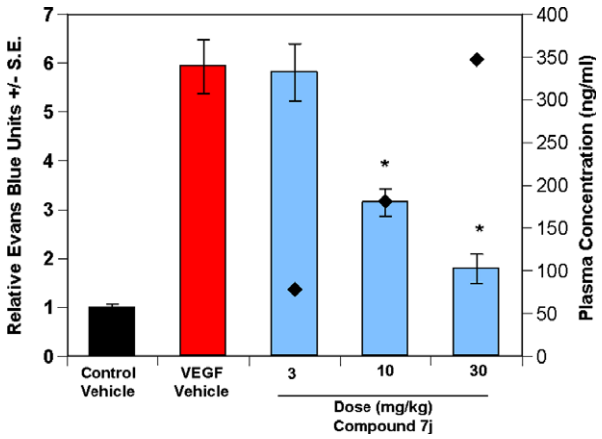

Scheme 4. Effect of compound **7j** in a VEGF-induced vascular permeability assay, $^{*}p < 0.0001$.

rat pharmacokinetic properties, and pharmacological activity of compound **7j**. Further evaluation in a VEGF-induced vascular permeability assay showed promising efficacy. Modification of this scaffold is currently under way with the aim of further optimizing potency and pharmacokinetic properties.

Acknowledgments

We thank Rebecca Bryant for her assistance with the vascular permeability assay. We are grateful to our colleagues Richard Lewis and Alan Cheng for helpful discussions regarding this manuscript.

Supplementary data

Supplementary data associated with this article can be found, in the online version, at doi:10.1016/j.bmcl.2008.07.080.

References and notes

1. (a) Folkman, J. *Ann. Surg.* **1972**, *175*, 409; (b) Ferrara, N. *Nat. Rev. Cancer* **2002**, *2*, 795.
2. (a) Hicklin, D. J.; Ellis, L. M. *J. Clin. Oncol.* **2005**, *23*, 1011; (b) Ferrara, N. *Endocr. Rev.* **2004**, *25*, 581.
3. Sakamoto, K. M. *Curr. Opin. Invest. Drugs* **2004**, *5*, 1329.
4. Ahman, T.; Eisen, T. *Clin. Cancer Res.* **2004**, *10*, 6388s.
5. (a) Manuscript in preparation.; (b) Potashman, M. H.; Kim, T.-S.; Bellon, S.; Booker, S.; Cheng, Y.; Kim, J. L.; Tasker, A.; Xi, N.; Xu, S.; Harmange, J.-C.; Borg, G.; Weiss, M.; Hodous, B. L.; Graceffa, R.; Buckner, W. H.; Masse, C. E.; Choquette, D.; Martin, M. W.; Germain, J.; Dipietro, L. V.; Chaffee, S. C.; Nunes, J. J.; Buchanan, J. L.; Habgood, G. J.; McGowan, D. C.; Whittington, D. A. PCT Int. Appl., WO 2005070891, 2005.
6. Belman, S.; Troll, W.; Teebor, G.; Mukai, F. *Cancer Res.* **1968**, *28*, 535.
7. Kubo, K.; Shimizu, T.; Ohyama, S.; Murooka, H.; Iwai, A.; Nakamura, K.; Hasegawa, K.; Kobayashi, Y.; Takahashi, N.; Takahashi, K.; Kato, S.; Izawa, T.; Isoe, T. *J. Med. Chem.* **2005**, *48*, 1359.
8. Charles, M. D.; Schultz, P.; Buchwald, S. L. *Org. Lett.* **2005**, *7*, 3965.
9. The enzyme and HUVEC proliferation assays were performed as previously described: Polverino, A.; Coxon, A.; Starnes, C.; Diaz, Z.; DeMelfi, T.; Wang, L.; Bready, J.; Estrada, J.; Cattley, R.; Kaufman, S.; Chen, D.; Gan, Y.; Kumar, G.; Meyer, J.; Neervannan, S.; Alva, G.; Talvenheimo, J.; Montestruque, S.; Tasker, A.; Patel, V.; Radinsky, R.; Kendall, R. *Cancer Res.* **2006**, *66*, 8715.

10. *c*Log*P* values were calculated employing software from ACD Labs (Advanced Chemistry Development Inc.).
11. La, D. S.; Harmange, J.-C.; Belzile, J.; Bready, J. V.; Coxon, A.; DeMelfi, T.; Doerr, N.; Estrada, J.; Flynn, J. C.; Flynn, S. R.; Graceffa, R. F.; Harriman, S. P.; Larrow, J. F.; Long, A. M.; Marin, M. W.; Morrison, M. J.; Patel, V. F.; Polverino, A. J.; Roveto, P. M.; Wang, L.; Weiss, M. W.; Whittington, D. A.; Teffera, Y.; Zhao, Z. *J. Med. Chem.* **2008**, *51*, 1695.
12. No inhibition of tissue growth is desired as the target is the selective inhibition of angiogenesis. See Ref. 9 for further detail.
13. All the compounds tested had F-HUVEC $IC_{50} > 1$ μM.
14. See Supporting information.
15. Liu, Y.; Gray, N. S. *Nat. Chem. Biol.* **2006**, *2*, 358.
16. Male Sprague–Dawley rats were dosed via femoral vein (intravenous, DMSO solution, dose 1 mg/kg) or via oral gavage (suspensions in Ora-Plus, pH adjusted to a range of 2.0–2.2 using methanesulfonic acid, dose 10 mg/kg). Concentrations of all formulations were selected to allow for dose volumes in accordance with the highest scientific, humane, and ethical principles as defined by IACUC (Institutional Animal Care and Use Committees). Serial blood samples were collected from jugular vein into heparized tubes for over a 12–24 h period. Plasma was separated by centrifugation, and the sample was prepared for analysis by protein precipitation with acetonitrile. Quantitation of the test compounds was accomplished by reverse phase liquid chromatography with mass spectral detection in multiple reaction monitoring mode, with an appropriate internal standard. Pharmacokinetic parameters such as clearance, volume of distribution, and terminal half-life were calculated by a noncompartmental method.
17. Vascular permeability was induced using a modified Miles assay Miles, A. A.; Miles, E. M. *J. Physiol.* **1952**, *118*, 228. HEK 293 cells over-expressing murine VEGF were used to induce vascular permeability in nude mice. 2×10^5 VEGF-expressing or vector control HEK 293 cells were mixed with Matrigel and injected subcutaneously on the ventral surface of nude mice. Approximately 24 h later, a single oral dose of compound or vehicle was administered. After 6 h, the mice received an intravenous injection of 0.1 mL 1% Evan's blue dye for 10 min prior to sacrifice. A 1 cm^2 piece of skin overlying the cells was harvested and placed in formamide at 60 °C overnight. The extracted Evan's blue dye was measured using a spectrophotometer at OD_{630}. Relative Evan's blue units refer to the % Evan's blue, as determined by the standard curve, multiplied by 10^4. Data represent mean ± standard error; $n = 5$ per group. Statistical analysis was performed by one-way ANOVA with Bonferroni-Dunn post-hoc test. $p < 0.0009$ was considered significant.